Dynamics of Hippocampal Neurogenesis in Adult Humans

Kirsty L. Spalding,[1],[8] Olaf Bergmann,[1],[8] Kanar Alkass,[1],[2] Samuel Bernard,[3] Mehran Salehpour,[4] Hagen B. Huttner,[1],[5] Emil Boström,[1] Isabelle Westerlund,[1] Céline Vial,[3] Bruce A. Buchholz,[6] Göran Possnert,[4] Deborah C. Mash,[7] Henrik Druid,[2] and Jonas Frisén[1],*

[1]Department of Cell and Molecular Biology
[2]Department of Oncology-Pathology
Karolinska Institutet, 171 77 Stockholm, Sweden
[3]Institut Camille Jordan, CNRS UMR 5208, University of Lyon, 69622 Villeurbanne, France
[4]Department of Physics and Astronomy, Ion Physics, Uppsala University, 751 20 Sweden
[5]Department of Neurology, University of Erlangen-Nuremberg, Schwabachanlage 6, 91054 Erlangen, Germany
[6]Center for Accelerator Mass Spectrometry, Lawrence Livermore National Laboratory, 7000 East Avenue L-397, Livermore, CA 94550, USA
[7]Department of Neurology, Miller School of Medicine, University of Miami, Miami, FL 33136, USA
[8]These authors contributed equally to this work
*Correspondence: jonas.frisen@ki.se
http://dx.doi.org/10.1016/j.cell.2013.05.002

SUMMARY

Adult-born hippocampal neurons are important for cognitive plasticity in rodents. There is evidence for hippocampal neurogenesis in adult humans, although whether its extent is sufficient to have functional significance has been questioned. We have assessed the generation of hippocampal cells in humans by measuring the concentration of nuclear-bomb-test-derived ^{14}C in genomic DNA, and we present an integrated model of the cell turnover dynamics. We found that a large subpopulation of hippocampal neurons constituting one-third of the neurons is subject to exchange. In adult humans, 700 new neurons are added in each hippocampus per day, corresponding to an annual turnover of 1.75% of the neurons within the renewing fraction, with a modest decline during aging. We conclude that neurons are generated throughout adulthood and that the rates are comparable in middle-aged humans and mice, suggesting that adult hippocampal neurogenesis may contribute to human brain function.

INTRODUCTION

New neurons integrate throughout life in the hippocampus and olfactory bulb of most mammals. The newborn neurons have enhanced synaptic plasticity for a limited time after their differentiation (Ge et al., 2007; Schmidt-Hieber et al., 2004), which is critical for their role in mediating pattern separation in memory formation and cognition in rodents (Clelland et al., 2009; Nakashiba et al., 2012; Sahay et al., 2011). It has long been debated whether adult neurogenesis decreased during primate evolution and whether there is sufficient generation of neurons in adult humans to contribute to brain function (Kempermann, 2012; Rakic,

1985). A seminal study by Eriksson et al., 1998, provided the only direct evidence to date for adult neurogenesis in humans, although it did not enable researchers to assess the number of new neurons generated or the dynamics of this process.

To estimate the extent of adult neurogenesis in humans, recent studies have quantified the number of cells expressing the neuronal precursor (neuroblast) marker doublecortin (DCX) in the subventricular zone, which gives rise to olfactory bulb neurons, and in the dentate gyrus of the hippocampus (Knoth et al., 2010; Sanai et al., 2011; Wang et al., 2011). Very similar dynamics have been revealed in these two regions, which contain a large number of neuroblasts shortly after birth that decreases sharply during the first postnatal year and then declines more moderately through childhood and adult life (Göritz and Frisén, 2012; Knoth et al., 2010; Sanai et al., 2011; Wang et al., 2011). The decrease in neuroblast numbers in the subventricular zone and their migratory path suggested that there is negligible, if any, adult olfactory bulb neurogenesis in humans (Arellano and Rakic, 2011; Sanai et al., 2011; Wang et al., 2011). Retrospective birth dating established that olfactory bulb neurons are as old as the individual, and, if there is any addition of neurons in the adult human olfactory bulb, less than 1% of the neurons are exchanged over a century (Bergmann et al., 2012). It appears unlikely that adult olfactory bulb neurogenesis has any functional significance in humans. The similar decline in neuroblast numbers in the subventricular zone and the hippocampus poses the question of whether there is postnatal hippocampal neurogenesis in humans to an extent that may have an impact on brain function.

Analysis of the number of neuronal progenitor cells gives an indirect indication of the possible extent of neurogenesis. However, it does not provide information as to whether neuroblasts differentiate and integrate as mature neurons. This is evident from the studies of the subventricular zone and olfactory bulb, where the generation of neuroblasts does not result in the detectable integration of new neurons in the olfactory bulb (Bergmann et al., 2012). The strategies used to study the generation of
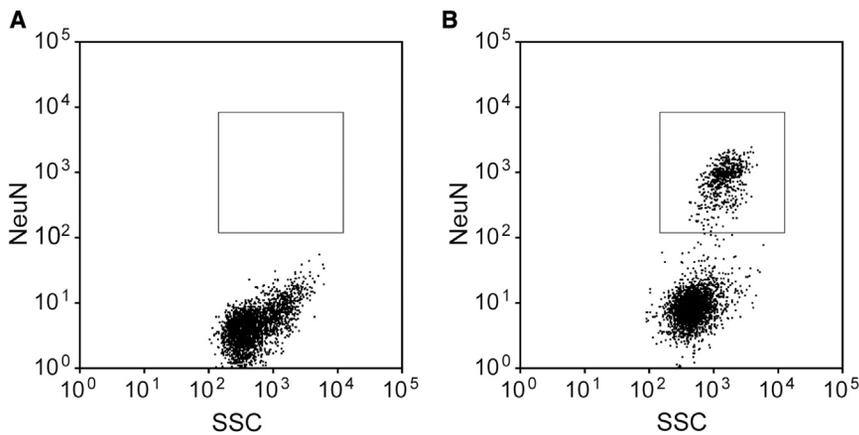
Figure 1. Isolation of Neuronal and Nonneuronal Nuclei from the Human Hippocampus

Cell nuclei were isolated from the human postmortem hippocampus and incubated with an isotype control antibody (A) or an antibody against the neuron-specific epitope (NeuN) (B), and the neuronal and nonneural populations were isolated by flow cytometry. The sorting gate for neuronal nuclei is indicated.

See also Figure S1.

mature neurons in experimental animals are not readily applicable to humans. To be able to study cell turnover dynamics in humans, we have developed a strategy to retrospectively birth date cells (Spalding et al., 2005a). This strategy takes advantage of the elevated atmospheric ^{14}C levels caused by above-ground nuclear bomb testing in 1955–1963 during the Cold War (De Vries, 1958; Nydal and Lövseth, 1965). Since the Partial Nuclear Test Ban Treaty in 1963, atmospheric levels of ^{14}C have declined because of uptake by the biotope and diffusion from the atmosphere (Levin and Kromer, 2004; Levin et al., 2010). ^{14}C in the atmosphere reacts with oxygen to form CO_2, which is taken up by plants in photosynthesis. When we eat plants, or animals that live off plants, we take up ^{14}C, meaning that atmospheric ^{14}C levels are mirrored in the human body at all times (Harkness, 1972; Libby et al., 1964; Spalding et al., 2005b). When a cell goes through mitosis and duplicates its chromosomes, it integrates ^{14}C in the synthesized genomic DNA with a concentration corresponding to that in the atmosphere at the time, creating a date mark in the DNA (Spalding et al., 2005a). The cumulative nature of ^{14}C integration makes the method especially suited for establishing the kinetics of slowly turning over cell populations. The accuracy of individual datings is approximately ±1.5 years (Spalding et al., 2005b), but higher accuracy is reached by integrating data from many independent measurements.

We have retrospectively birth dated hippocampal cells, and we provide an integrated model for adult hippocampal neurogenesis in humans. We report that there is substantial neurogenesis in the human hippocampus throughout life, to an extent comparable to that in the middle-aged mouse, thus supporting the idea that adult hippocampal neurogenesis may contribute to human brain function.

RESULTS

Retrospective Birth Dating of Cells from the Human Hippocampus

Cell nuclei were isolated by gradient centrifugation from dissected human postmortem hippocampi. The nuclei were incubated with antibodies against the neuron-specific nuclear epitope NeuN, and neuronal and nonneuronal nuclei were isolated by flow cytometry (Figure 1 and Figure S1 available online)

(Bergmann et al., 2012; Bhardwaj et al., 2006; Spalding et al., 2005a). The ^{14}C concentration in genomic DNA from hippocampal neurons (n = 55) and nonneuronal cells (n = 65) was measured by accelerator mass spectrometry (AMS) in subjects 19–92 years of age (^{14}C data are given in Table S1).

Standard AMS analysis requires samples corresponding to about 1 mg of carbon. The total amount of carbon in genomic DNA samples from hippocampal cell populations, after cell sorting and purifications steps, is typically in the range 10–20 μg, necessitating a different approach. Consequently, we developed an experimental method with a sample preparation setup and laboratory procedure to address various critical issues, including reliability and accuracy (Salehpour et al., 2013).

To infer the cell turnover dynamics in the adult hippocampus, we fitted several mathematical models, or scenarios, with increasing detail to the ^{14}C data. All scenarios were based on birth and death processes by which cells can die or be added to a cell population. A scenario defines a set of rules for how cells are born, die, or renew; i.e., it sets whether there should be more, less, or equal amounts of birth and death and which cells will die preferentially or renew, etc. For each of these scenarios, a set of parameters quantifies the extent of renewal. The mathematical model tracks the chronological age of each cell and the age of the person with a variable $n(t, a)$, with the cell density (units in cells per year) of age a in a person age t. The evolution of the cell density is given by a biological transport equation, which moves cells along age as time progresses with a loss term accounting for cell death:

$$\frac{\partial n(t, a)}{\partial t} + \frac{\partial n(t, a)}{da} = -\gamma(t, a)n(t, a).$$

An initial condition describing the cell population at birth and a boundary condition describing how new cells are added are supplemented to the transport equation to solve the problem fully (equations are given in the Extended Experimental Procedures). Solving the problem allows the prediction of the ^{14}C level for a sample by integrating the solution $n(t, a)$ along the atmospheric ^{14}C curve between the birth and death of the individual. By comparing the model prediction to all neuronal or nonneuronal cell data, best parameter sets for each scenario were found. The best scenarios were selected on the basis of Akaike information criterion (AIC); i.e., their goodness of fit and their level of
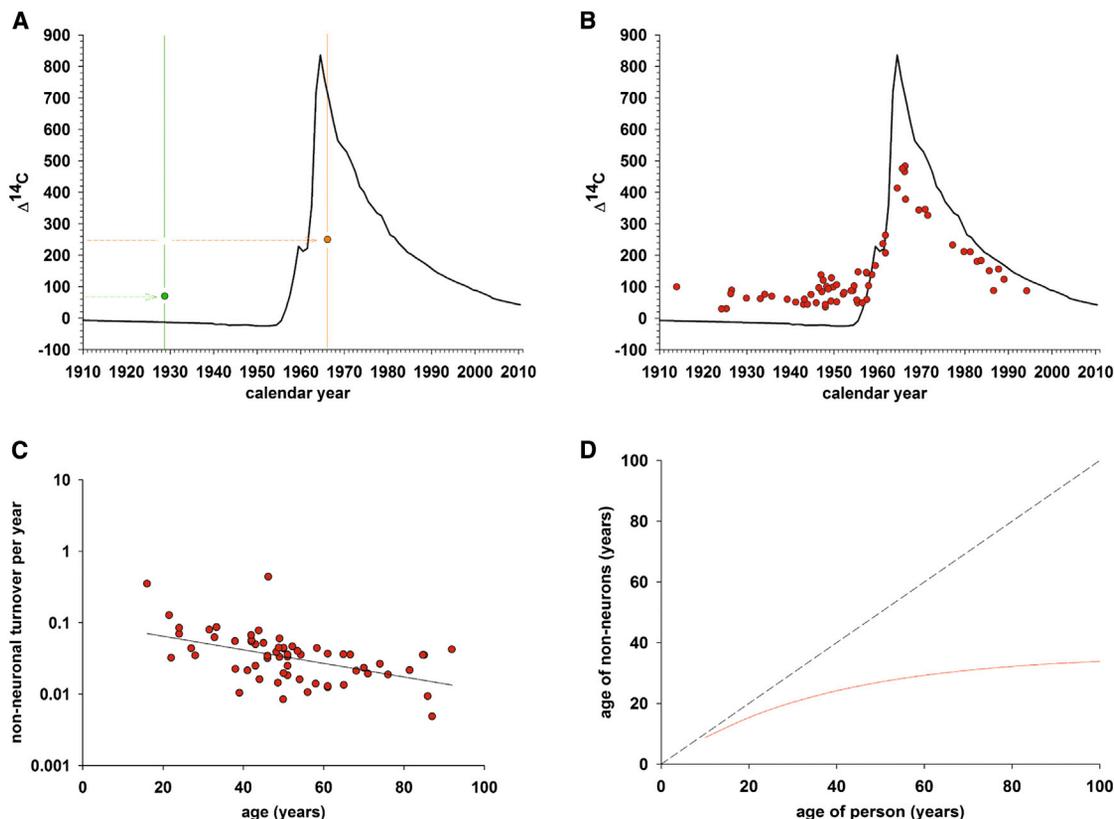
Figure 2. Turnover Dynamics of Nonneuronal Cells
(A) Schematic illustration of the representation of the measured ^{14}C concentration in genomic DNA. The black line indicates the ^{14}C concentration in the atmosphere at different time points in the last century. Individually measured ^{14}C concentrations in the genomic DNA of human hippocampal cells are plotted at the time of the subject's birth (vertical lines), before (green dot) or after the ^{14}C bomb spike (orange dot). ^{14}C concentrations above the bomb curve (subjects born before the bomb peak) and data points below the bomb curve (subjects born after the nuclear tests) indicate cellular turnover.
(B) The ^{14}C concentrations of genomic DNA from nonneuronal cells demonstrate postnatal cell turnover in subjects born before and after the bomb spike.
(C) Individual turnover rates for Nonneuronal cells computed on the basis of individual data fitting. Individual turnover rate calculations are sensitive to deviations in measured ^{14}C and values <0.001 or >1.5 were excluded from the plot, but the full data are given in Table S1.
(D) Nonneuronal average cell age estimates of cells within the renewing fraction are depicted (red curve). The dashed line represents a no-cell-turnover scenario. See also Figure S2 and Table S2.

detail. For scenario A (constant turnover) and scenario 2POP (constant turnover in a fraction of cells), individual turnover rates could also be estimated.

Turnover of Nonneuronal Cells in the Adult Human Hippocampus

First, we assessed the turnover dynamics of nonneuronal (NeuN−) cells in the human hippocampus. The ^{14}C concentration in genomic DNA corresponded to time points after the birth of the individuals (Figures 2A and 2B), establishing the turnover of nonneuronal cells in the human hippocampus. Mathematical modeling of ^{14}C data allowed a detailed analysis of the dynamics of cell turnover (Bergmann et al., 2009; Bergmann et al., 2012; Spalding et al., 2008). By fitting the models to the data, we can infer how much cell renewal is needed to reproduce the observed ^{14}C levels and whether the renewal is restricted to a subpopulation (see Figure S2 and the Extended Experimental Procedures). The best model, based on AIC, was scenario 2POP, in which a fraction of the population is renewing and the

other is not. In this scenario, cells within the renewing fraction are set to turn over at a constant rate throughout life. This scenario indicated that a large proportion of the nonneuronal cells (51%, 95% confidence interval [CI] [22%–88%]) are continuously exchanged. The median turnover rate within the subpopulation of nonneuronal cells undergoing exchange is 3.5% per year (Figure 2C and Table S2). Individual turnover estimates suggest that there is a decline in the turnover of nonneuronal cells during aging (r = −0.35, p = 0.04). The average age of nonneuronal cells within the renewing fraction at different ages of an individual is shown in Figure 2D.

Hippocampal Neurogenesis in Adult Humans

Next, we analyzed the ^{14}C concentration in neuronal genomic DNA. One can draw several conclusions regarding hippocampal neurogenesis from the raw data (Figure 3). First, the ^{14}C concentration in genomic DNA of hippocampal neurons corresponds to the concentration in the atmosphere after the birth of the individual, confirming the postnatal generation of hippocampal neurons
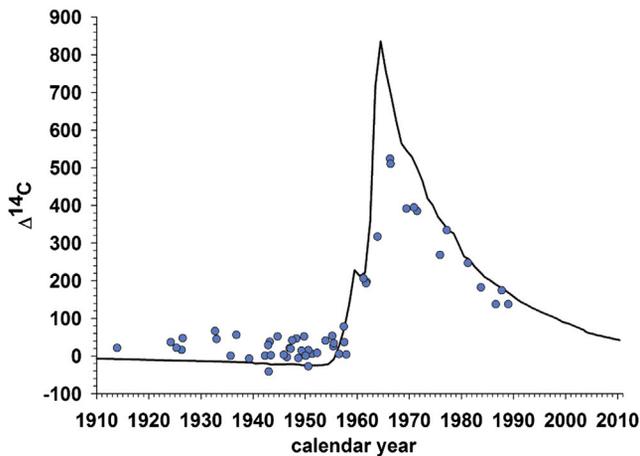
Figure 3. Hippocampal Neurogenesis in Adult Humans
[14]C concentrations in hippocampal neuron genomic DNA correspond to a time after the date of birth of the individual, demonstrating neurogenesis throughout life.

in humans (Eriksson et al., 1998). This finding is in contrast to cortical and olfactory bulb neurons, which are not exchanged postnatally to a detectable degree in humans, and ^{14}C levels correspond to the time around the birth of the individual (Bergmann et al., 2012; Bhardwaj et al., 2006; Spalding et al., 2005a). Second, the oldest studied subjects had higher ^{14}C concentrations in neuronal DNA than were present in the atmosphere before 1955 (Figure 3). This finding establishes that there has been DNA synthesis after 1955, indicating hippocampal neurogenesis into at least the fifth decade of life (the oldest individual was 42 years old in 1955). Third, the rather uniformly elevated levels of ^{14}C in individuals born before the onset of the nuclear bomb tests indicate that there can be no dramatic decline in hippocampal neurogenesis with age; if there was a substantial decrease in neurogenesis during aging, then individuals born longer before the rise in atmospheric ^{14}C would have incorporated less of the elevated ^{14}C levels present after 1955. Fourth, individuals born before the onset of nuclear bomb tests have lower ^{14}C levels in hippocampal neuron DNA than at any time after 1955, establishing that, although some neurons are generated postnatally, the hippocampus is heterogeneous, and a large subset of hippocampal neurons is not exchanged postnatally. Thus, it is evident from the raw data that there is substantial generation of hippocampal neurons in humans, restricted to a subpopulation, without any dramatic decline during adulthood.

A Large Proportion of Hippocampal Neurons Are Subject to Turnover

Adult hippocampal neurogenesis in mammals is restricted to the dentate gyrus (Kempermann, 2012). With the current sensitivity of AMS, it is not possible to separately carbon date neurons from subdivisions of the human hippocampus. However, neuroblasts and BrdU-labeled neurons have only been demonstrated in the dentate gyrus in adult humans (Eriksson et al., 1998; Knoth et al., 2010), indicating that neuronal turnover is also restricted to the dentate gyrus in humans. The term "turnover of neurons" does not imply that individual neurons that are lost are replaced

by new neurons taking over their function but that there is an exchange of neurons at the population level. It was evident from the raw data (Figure 3) that not all hippocampal neurons are exchanged postnatally in humans. Models that allowed two compartments, one population that turns over constantly and one that is nonrenewing, fitted the data much better than any other model (see the Extended Experimental Procedures). Scenario 2POP indicates that the size of the cycling neuronal population constitutes 35% (95% CI [12%–63%]) of hippocampal neurons (Figure 4A), corresponding to slightly less than the proportion of hippocampal neurons that constitute the dentate gyrus in humans (see below). This finding indicates that the vast majority of dentate gyrus neurons are subject to exchange in humans, differing from the situation in the mouse, in which approximately 10% of the dentate gyrus neurons are subject to exchange (Imayoshi et al., 2008; Santos et al., 2007). The proportion of hippocampal neurons that are exchanged has not been addressed in other species.

It is possible that cells in the hippocampus form a heterogeneous population in terms of renewal. A scenario with a continuum of turnover rates was used to assess the heterogeneity of the neuronal and nonneuronal cell populations (scenario XPOP in Extended Experimental Procedures). The modeling indicates that the neuronal subpopulation that is turning over in the hippocampus is rather homogeneous and confers to one mode of exchange (Figure 4A). The nonneuronal cells form a heterogeneous group of cells, consisting mainly of astrocytes, microglia, and oligodendrocyte-lineage cells but also containing several smaller populations of, for example, leukocytes and blood-vessel-associated endothelial and perivascular cells. In line with this, models that allowed subpopulations to have different turnover dynamics fitted the nonneuronal data best. The nonneuronal cells appear more heterogeneous than the neurons, some nonneuronal cells having high turnover rates and some having very low ones (Figure 4B).

The Rate of Neuronal Turnover in the Human Hippocampus

Given that the majority of hippocampal neurons are not exchanged, the average age of hippocampal neurons increases with the age of the individual, which may give the false impression that the turnover rate decreases sharply during aging. However, when taking into account that neurogenesis is restricted to a subpopulation, individual estimates of turnover rates indicate a more modest decline in turnover with aging within this population (Figures 5A and S3 and Table S3; r = −0.31, p = 0.03, scenario 2POP in Extended Experimental Procedures). The median turnover rate of neurons within the renewing subpopulation is 1.75% per year during adulthood, corresponding to approximately 700 new neurons per day in each hippocampus or 0.004% of the dentate gyrus neurons per day in the human hippocampus. The turnover rate of hippocampal neurons is not significantly different between men and women (p = 0.41, ANOVA). The average age of neurons within the renewing fraction at different ages of an individual is shown in Figure 5B.

Comparing the turnover rates between the full neuronal and nonneuronal hippocampal populations reveals a significantly higher turnover rate within the nonneuronal compartment
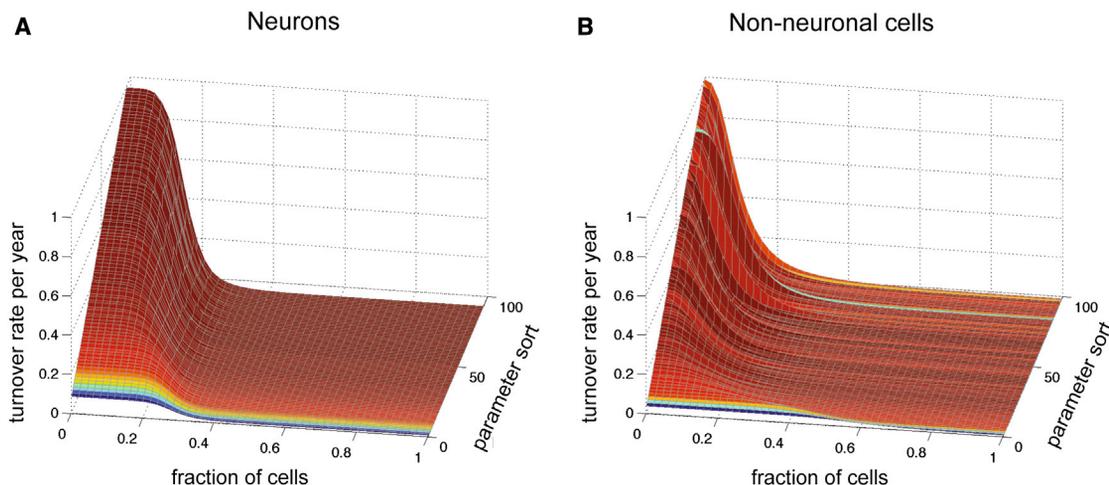
Figure 4. Subpopulation Dynamics of Hippocampal Neurons and Nonneurons
(A) The Hill function indicates that the fraction of neurons being exchanged is homogenous and confers to one mode of exchange.
(B) In line with a nonneuronal population comprised of several cell types, the Hill function indicates that the nonneuronal cells form a heterogeneous group, some subpopulations having high turnover rates and some having very low ones. The z axis indicates different possible solutions compatible with the data. Only solutions with a good fit are shown, and those with the highest probability are indicated in red. Solutions with a lower probability in are indicated in blue.

($p < 2 \times 10^{-5}$, Wilcoxon signed-rank test, scenario A in Extended Experimental Procedures). This finding is largely explained by a larger subset of cells turning over within the nonneuronal population than within the neuronal population, and, when comparing the turnover rates specifically within the respective subpopulations that are subject to cellular exchange, there was no significant difference in turnover rates between the neuronal and nonneuronal populations ($p = 0.054$, Wilcoxon signed-rank test, scenario 2POP in Extended Experimental Procedures). However, given that nonneuronal cells are more abundant than neurons in the human hippocampus (Figure 1A), a larger number of nonneuronal cells in absolute numbers are generated.

There was no correlation between the neuronal and nonneuronal turnover rates within individuals older than 50 years ($r = -0.14$, $p = 0.58$, scenario 2POP in Extended Experimental Procedures), suggesting that the generation of these different cell types is regulated independently, as in the mouse (Steiner et al., 2004). However, there was a correlation in young individuals (<50 years, $r = -0.62$, $p = 0.003$). The interindividual variation in the turnover rate of neurons and nonneuronal cells in the hippocampus is similar, having a median absolute deviation of 0.0226 and 0.0158 per year, respectively. The interindividual variation may appear largest in the younger subjects, but this is a consequence of the shallow slope of the atmospheric ^{14}C levels in recent times, which provides less resolution and, therefore, introduces higher variability.

An Integrated Model of Neuronal Dynamics in the Human Hippocampus
The determination of the fraction of neurons that is subject to exchange in the human hippocampus and their turnover rate makes it possible to infer the age of the full complement of neurons in individuals of different ages. The hippocampus is a mosaic of neurons of different ages, given the large fraction of cells remaining from development and neurons generated at

different times throughout life. Stereological quantifications have revealed a decrease in the number of hippocampal neurons during aging in humans, the dentate gyrus being least affected (Figure S4). A relative increase in the proportion of neurons in the renewing fraction with age fits the ^{14}C data well.

The most detailed model, scenario 2POPEd, provides a global picture of the dynamics of neuronal turnover. Nonrenewing neurons die without being replaced, resulting in a slow decrease in neuron level throughout life. Within the renewing neuron population, young cells die faster, leading to a neuron age distribution with fewer middle-aged cells than would be expected if all neurons were as likely to be replaced. One observation from the modeling is that adult-born neurons are preferentially lost and do not survive as long as the neurons generated during development. The half-life of a neuron in the renewing fraction is 7.1 years—10× shorter than in the nonrenewing fraction. Although it is known that adult-born neurons integrate long term in rodents, whether they last for the remainder of the animal's life has not been studied, although the available data are compatible with a preferential loss of adult-born neurons (Imayoshi et al., 2008; Kempermann et al., 2003; Ninkovic et al., 2007). The integrated model of the dynamics of hippocampal neuron numbers and exchange in humans is shown in Figure 6.

DISCUSSION

Newborn neurons in the adult hippocampus have distinct features for a limited period after their differentiation that give them a key role in pattern separation and cognitive adaptability in rodents. We have birth dated hippocampal cells in order to assess whether adult neurogenesis occurs to a significant extent in adult humans, and we provide a detailed view of the cell turnover dynamics. There is substantial neurogenesis throughout life in the human hippocampus, and only a modest decline in neurogenesis occurs during aging. There is a
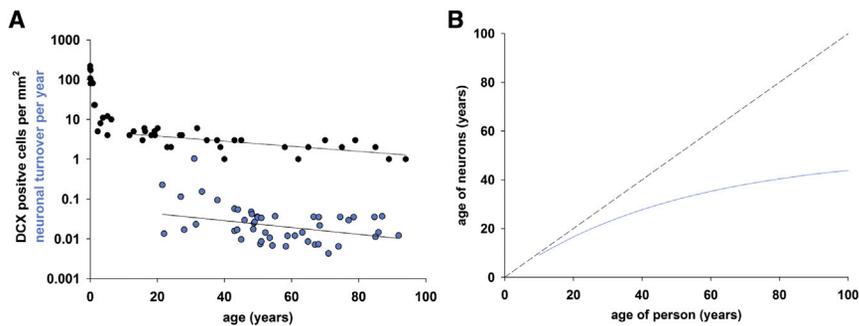
Figure 5. Neuronal Turnover Dynamics in the Human Hippocampus

(A) Individual turnover rates for neuronal cells within the renewing fraction were computed on the basis of individual data fitting. The number of DCX-positive cells per mm^2 in the dentate gyrus (data from Knoth et al., 2010) shows a similar modest decline during adult ages as the computed neuronal turnover rates. Straight lines depict linear regression curves, and the regression line for DCX cell counts was calculated for individuals 10 years and older. Individual turnover rate calculations are sensitive to deviations in measured ^{14}C and values <0.001 or >1.5 were excluded from the plot, but the full data are given in Table S1.

(B) The average age of the neurons within the renewing fraction (blue curve). The dashed line represents the no-cell-turnover scenario. See also Figure S3 and Table S3.

preferential loss of adult-born neurons, and a larger proportion of hippocampal neurons are subject to exchange in humans in comparison to the mouse. Nonneuronal cells have more heterogeneous turnover dynamics than hippocampal neurons.

It is important to consider whether DNA repair may contribute to ^{14}C integration in hippocampal cells. DNA damage and repair are largely restricted to proliferating cells and are believed to be several orders of magnitude below the level that is detectable by ^{14}C dating in postmitotic cells (Spalding et al., 2005a). DNA repair during cell proliferation will not affect the assessment of cell generation, given that ^{14}C integrates in DNA at a concentration corresponding to that in the atmosphere during mitosis. We have not found any measurable ^{14}C integration in the DNA of cortical, cerebellar, or olfactory bulb neurons over many decades in humans (Bergmann et al., 2012; Bhardwaj et al., 2006; Spalding et al., 2005a). Not even neurons surviving at the perimeter of an ischemic cortical stroke, a situation where there is substantial DNA damage and repair, incorporate sufficient ^{14}C to be detected (H.B.H., O.B., M.S., G.P., and J.F., our unpublished data). The dynamics of ^{14}C integration in the DNA of hippocampal neurons does not appear to be compatible with any pattern of DNA repair previously described; a large fraction of hippocampal neurons (35%) would have to exchange their entire genome by DNA repair during the lifetime of an individual, whereas there would be no detectable DNA repair in the remaining hippocampal neurons. In contrast, the number of neuroblasts reported in the adult human dentate gyrus (Knoth et al., 2010) is sufficient to give rise to the number of new neurons indicated by the ^{14}C analysis, and the decline in neurogenesis closely parallels the decrease in the number of neuroblasts (Figure 5A). Thus, the ^{14}C concentration in genomic DNA of hippocampal neurons is likely to accurately reflect neurogenesis.

Retrospective birth dating reveals that what appears as small numbers of neuroblasts present in adulthood (Knoth et al., 2010) give rise to a substantial number of new neurons over time in the hippocampus. In this context, it is interesting that the similar density of neuroblasts in the subventricular zone to that in the hippocampal dentate gyrus does not result in any detectable addition of new neurons to the olfactory bulb (Bergmann et al., 2012; Göritz and Frisén, 2012; Knoth et al., 2010; Sanai et al., 2011; Wang et al., 2011). Thus, the lack of olfactory bulb neurogenesis appears to be a consequence of an absence of migration and/or

integration of new neurons in the olfactory bulb rather than a lack of generation of neuroblasts.

There are some distinct differences in the pattern of adult hippocampal neurogenesis in humans compared to that in rodents, in which this process has been most extensively characterized. First, a much larger proportion of hippocampal neurons are subject to exchange in humans. In mice, 10% of the neurons in the dentate gyrus are added in adulthood and subject to exchange (Imayoshi et al., 2008; Ninkovic et al., 2007). In humans, approximately one-third of the hippocampal neurons turn over, corresponding to the vast majority of the dentate gyrus neurons. Second, although hippocampal neurogenesis declines with age in both rodents and humans, the relative decline during adulthood appears smaller in humans in comparison to mice. Comparisons of the kinetics of the age-dependent decline in hippocampal neurogenesis between different species have revealed a similar chronology rather than correlating to developmental milestones (Amrein et al., 2011). In line with this, the most dramatic decrease in the number of neuroblasts in the dentate gyrus occurs during the first postnatal months in both mice and humans (Ben Abdallah et al., 2010; Knoth et al., 2010). An effect of this is that young adult mice are still in the most steeply declining phase of neurogenesis, making the relative decrease in neurogenesis during adult life much larger in mice than in humans. Although there is an approximately 10-fold decrease in neurogenesis from 2 to 9 months of age in mice (Ben Abdallah et al., 2010), there is an approximate 4-fold decline during the entire adult lifespan in humans (Figure 5A). Third, the impact of adult neurogenesis on the total number of neurons in the dentate gyrus differs between rodents and humans. Hippocampal neurogenesis in mice and rats is additive and results in a net increase in the number of dentate gyrus neurons with age (Bayer, 1985; Imayoshi et al., 2008; Kempermann et al., 2003; Ninkovic et al., 2007). This is not the case in humans, where there is a net loss of dentate gyrus neurons during adult life. Although the decrease in neuronal numbers is less pronounced in the dentate gyrus than in other subdivisions of the human hippocampus, the generation of new neurons does not keep up with neuronal loss (Figure 6). Computational models have indicated that the addition of new neurons to the circuitry, along with loss of older redundant cells and enhanced synaptic plasticity, can maximize the effect of the new neurons, whereas an isolated exchange of neurons
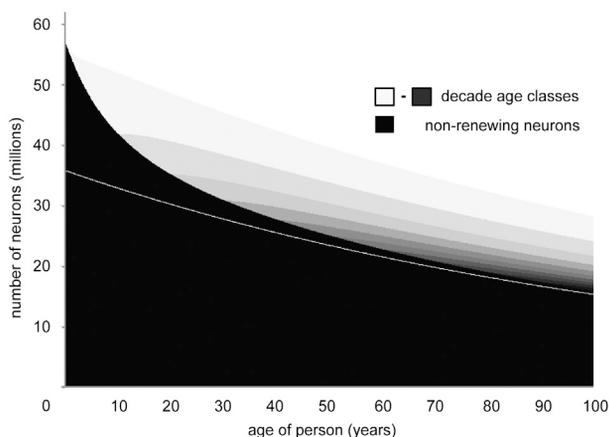
Figure 6. An Integrated Model of the Number and Age of Neurons in the Human Hippocampus

A schematic illustration of the number of neurons in the dentate gyrus (above the white line) and other subdivisions of the hippocampus (below the white line) and the age of neurons within the dentate gyrus at different ages. The total number of neurons declines with age in the hippocampus, though the dentate gyrus is relatively spared. The dentate gyrus is composed of a declining fraction of cells generated during development (black), which is gradually replaced by postnatally generated cells. For a given age of the person, postnatally generated cells are shown with different shades of gray indicating decade intervals, the lightest gray being cells generated during the last decade, and cells one shade darker being generated 10 to 20 years ago, etc. This way, at age 15 among postnatally generated cells, only cells generated 0 to10 years ago and 10 to 20 years ago are present. Read vertically for a fixed age of the person, the cell age distribution goes from oldest cells (black) to the youngest ones (light gray). Read horizontally, the fraction of adult-born cells (nonblack) increases with age. The model is based on scenario 2POPEd. The figure was generated with the following parameters: initial fraction of renewing neurons, 0.31; death rate of the nonrenewing neurons, 0.0035 per year; death rate of newborn neurons, 0.11 per year; and cell age at which the death rate has reduced by half, 19 years. The parameter set was selected among the 3% best out of 3×10^5 parameter sets explored with a Markov chain Monte Carlo algorithm and consistent with scenario 2POP.

See also Figure S4.

would have less influence (Appleby et al., 2011). The adult generation of neurons serves to uphold a pool of neurons with specific functional properties rather than replacing individual neurons that are lost. Therefore, the continuous generation of new neurons in the adult human hippocampus may have an additive role functionally in the circuitry, although more neurons are lost than generated.

Can the number of new neurons generated in the adult human hippocampus have functional significance? An indication of this may be gained by comparing the extent of adult neurogenesis in humans with that in other species, in particular the mouse, in which most experiments on the function of adult hippocampal neurogenesis have been carried out. It is difficult to make direct comparisons because there are several factors influencing the potential impact of newborn neurons that may vary between species; for example, the total number of cells in the circuitry and for how long newborn neurons have distinct features. The best measure of adult neurogenesis when comparing across species may be the relative proportion of newborn to old neurons (Kempermann, 2012). We conclude that 0.004% of the dentate

gyrus neurons are exchanged daily in adult humans, which can be compared to 0.03%–0.06% per day in 2-month-old mice and 0.004%–0.02% per day in 5- to 16-year-old macaque monkeys (Jabès et al., 2010; Kempermann et al., 1997; Kornack and Rakic, 1999). Hippocampal neurogenesis has been estimated to decrease approximately 10-fold between 2 and 9 months of age in the mouse (Ben Abdallah et al., 2010), indicating that the rate of neurogenesis in adult humans may correspond to that of a 9-month-old mouse. Along with the extended period of immature features of the adult-born neurons in nonhuman primates (Kohler et al., 2011), and potentially humans, the relative proportion of adult-born neurons with unique functions in the human hippocampus may not be smaller than that in a middle-aged mouse. Therefore, the extent of neurogenesis in the adult human hippocampus may be sufficient to convey similar functions as in the mouse, in which adult neurogenesis is important for cognitive adaptability.

Adult-born hippocampal neurons have enhanced synaptic plasticity for a period of time after their differentiation (Ge et al., 2007; Schmidt-Hieber et al., 2004). This, along with the fact that the dentate gyrus acts as a bottleneck in the network, allows a small proportion of neurons to have a substantial influence on the circuitry and hippocampal function. The new neurons are required for efficient pattern separation and the ability to distinguish and store similar experiences as distinct memories, whereas the old granule cells are necessary for pattern completion, which serves to associate similar memories to each other (Clelland et al., 2009; Nakashiba et al., 2012; Sahay et al., 2011). Failing pattern separation may result in generalization, a common feature in anxiety and depression in humans (Kheirbek et al., 2012). There are a number of indications that implicate reduced neurogenesis in psychiatric disease, but it has been difficult to explore whether there is a link in humans (Eisch and Petrik, 2012). We find considerable interindividual variation in this study, and the assessment of hippocampal neurogenesis, along with the reconstruction of medical histories, may reveal whether reduced neurogenesis is associated with psychiatric disease in humans.

EXPERIMENTAL PROCEDURES

Tissue Collection

Nuclei Isolation

Tissue samples were thawed and Dounce homogenized in 10 ml lysis buffer (0.32 M sucrose, 5 mM CaCl$_2$, 3 mM magnesium acetate, 0.1 mM EDTA, 10 mM Tris-HCl [pH 8.0], 0.1% Triton X-100, and 1 mM DTT). Homogenized samples were suspended in 20 ml of sucrose solution (1.7 M sucrose, 3 mM magnesium acetate, 1 mM DTT, and 10 mM Tris-HCl [pH 8.0]), layered onto

a cushion of 10 ml sucrose solution, and centrifuged at 36,500 × g for 2.4 hr at 4°C. The isolated nuclei were resuspended in nuclei storage buffer (10 mM Tris [pH = 7.2], 2 mM $MgCl_2$, 70 mM KCl, and 15% sucrose) for consecutive immunostaining and flow cytometry analysis.

FACS Sorting and Analysis

Isolated nuclei were stained with mouse NeuN (A-60) (Millipore, 1:1,000). NeuN (A-60) antibody was directly conjugated to Alexa 647 (Alexa Flour 647 Antibody Labeling Kit, Invitrogen). Flow cytometry analyses and sorting were performed with a BD FACSDiva (BD Biosciences) or MoFlo XDP (Beckman Coulter) high-speed sorter. Fluorescence-activated cell sorting (FACS) correction for sort purity is detailed in the Extended Experimental Procedures. The FACS gating strategy for sorts is shown in Figures 1 and S1.

Correction for FACS impurities

In the case that the sorting purity was less than 100%, FACS impurities were corrected for by solving the following equation system for $\Delta 14C_{nonneurons\_corrected}$ and $\Delta 14C_{neurons\_corrected}$ ($y_{impurity\_nonneurons}$ and $x_{impurity\_neurons}$ are given in percentages). Corrected values are shown in Table S1.

$$\Delta 14C_{nonneurons\_measured} * 100 = \left(100 - y_{impurity\_non-neurons}\right)$$
$$* \Delta 14C_{nonneurons\_corrected} + y_{impurity\_non-neurons} * \Delta 14C_{neurons\_corrected} \quad (1)$$

$$\Delta 14C_{neurons\_measured} * 100 = \left(100 - x_{impurity\_neurons}\right)$$
$$* \Delta 14C_{neurons\_corrected} + x_{impurity\_neurons} * \Delta 14C_{nonneurons\_corrected} \quad (2)$$

DNA Purification

All experiments were carried out in a clean room (ISO8) to prevent any carbon contamination of the samples. All glassware was prebaked at 450°C for 4 hr. DNA isolation was performed according to a modified protocol from Miller et al., 1988. Then, 500 μl DNA lysis buffer (100 mM Tris [pH 8.0], 200 mM NaCl, 1% SDS, and 5 mM EDTA) and 6 μl Proteinase K (20 mg/ml) were added to the collected nuclei and incubated overnight at 65°C. RNase cocktail was added (Ambion) and incubated at 65°C for 1 hr. Half of the existing volume of 5 M NaCl solution was added, and the mixture was agitated for 15 s. The solution was spun down at 13,000 rpm for 3 min. The supernatant containing the DNA was transferred to a 12 ml glass vial. We added 3× the volume of absolute ethanol and inverted the glass vial several times to precipitate the DNA. The DNA precipitate was washed three times in DNA-washing solution (70% ethanol [v/v] and 0.1 M NaCl) and transferred to 500 μl DNase- and RNase-free water (Gibco and Invitrogen, respectively). The DNA was quantified, and DNA purity was verified by UV spectroscopy (NanoDrop).

Accelerator Mass Spectrometry

All AMS analyses were performed blind to age and origin of the sample. Purified DNA samples suspended in water were lyophilized to dryness. To convert the DNA sample into graphite, we added excess CuO to each dry sample, and the tubes were evacuated and sealed with a high-temperature torch. Tubes were placed in a furnace set at 900°C for 3.5 hr in order to combust all carbon to CO2. The evolved CO2 was purified, trapped, and reduced to graphite in the presence of iron catalyst in individual reactors at 550°C for 6 hr. Graphite targets were measured independently at the Center for Accelerator Mass Spectrometry at the Lawrence Livermore National Laboratory (Fallon et al., 2007) and the Department of Physics and Astronomy, Ion Physics, of Uppsala University (Salehpour et al., 2013). Large CO_2 samples (>100 μg) were split, and $\delta^{13}C$ was measured by stable isotope ratio mass spectrometry, which established the $\delta^{13}C$ correction to −22.3‰ ± 0.5‰ (1 SD), which was applied for all samples. Corrections for background contamination introduced during sample preparation were made as described previously (Brown and Southon, 1997; Hua et al., 2004; Santos et al., 2007). The measurement error was determined for each sample and ranged between ±4‰ and ±12‰ (1 SD) $\Delta^{14}C$ for the large sample and small samples (10 μgC), respectively. All ^{14}C data are reported as decay-corrected $\Delta^{14}C$ or fraction modern.

Statistics and Mathematical Modeling

The statistical methodologies used in this paper are as follows. The median, which is robust in the presence of outliers, was chosen as a location parameter. For the comparison of two matched samples, we used a Wilcoxon signed-rank test, which tests the median difference between the pairs to be zero. Because the median is used as a location parameter, we decided to measure the deviation in terms of absolute deviation from median. The link between two quantitative variables was assessed with a correlation measure and test, whereas the influence of a qualitative variable on a quantitative variable was measured with ANOVA.

Mathematical modeling was based on birth and death processes and renewal equations representing different scenarios performed essentially as described previously (Bergmann et al., 2009) and as outlined in detail in the Extended Experimental Procedures. These models were integrated along the atmospheric ^{14}C curve in order to yield a prediction of the DNA ^{14}C concentration. Nonlinear least-square and Markov chain Monte Carlo algorithms were used to estimate the best global parameters for each scenario for the neuronal and the nonneuronal cell samples. The AIC was used to compare the different scenarios. Individual turnover rates were estimated from scenarios A and 2POP for all the samples. Scenario A provided a direct turnover rate estimate for each sample. However, for scenario 2POP, the fraction of renewing cells had to be fixed in order to uniquely determine the turnover rates. The fraction was set to 0.35 for the neurons and 0.55 for the nonneuronal cells.

SUPPLEMENTAL INFORMATION

Supplemental Information includes Extended Experimental Procedures, four figures, and three tables and can be found with this article online at http://dx.doi.org/10.1016/j.cell.2013.05.002.

REFERENCES

Amrein, I., Isler, K., and Lipp, H.P. (2011). Comparing adult hippocampal neurogenesis in mammalian species and orders: influence of chronological age and life history stage. Eur. J. Neurosci. *34*, 978–987.

Appleby, P.A., Kempermann, G., and Wiskott, L. (2011). The role of additive neurogenesis and synaptic plasticity in a hippocampal memory model with grid-cell like input. PLoS Comput. Biol. *7*, e1001063.

Arellano, J.I., and Rakic, P. (2011). Neuroscience: Gone with the wean. Nature *478*, 333–334.

Bayer, S.A. (1985). Neuron production in the hippocampus and olfactory bulb of the adult rat brain: addition or replacement? Ann. N Y Acad. Sci. *457*, 163–172.

Ben Abdallah, N.M., Slomianka, L., Vyssotski, A.L., and Lipp, H.P. (2010). Early age-related changes in adult hippocampal neurogenesis in C57 mice. Neurobiol. Aging *31*, 151–161.

Bergmann, O., Bhardwaj, R.D., Bernard, S., Zdunek, S., Barnabé-Heider, F., Walsh, S., Zupicich, J., Alkass, K., Buchholz, B.A., Druid, H., et al. (2009). Evidence for cardiomyocyte renewal in humans. Science *324*, 98–102.

Bergmann, O., Liebl, J., Bernard, S., Alkass, K., Yeung, M.S., Steier, P., Kutschera, W., Johnson, L., Landén, M., Druid, H., et al. (2012). The age of olfactory bulb neurons in humans. Neuron *74*, 634–639.

Bhardwaj, R.D., Curtis, M.A., Spalding, K.L., Buchholz, B.A., Fink, D., Björk-Eriksson, T., Nordborg, C., Gage, F.H., Druid, H., Eriksson, P.S., and Frisén, J. (2006). Neocortical neurogenesis in humans is restricted to development. Proc. Natl. Acad. Sci. USA *103*, 12564–12568.

Brown, T.A., and Southon, J.R. (1997). Corrections for contamination background in AMS 14C measurements. Nucl Instrum Methods Phys Res Sect B *123*, 208–213.

Clelland, C.D., Choi, M., Romberg, C., Clemenson, G.D., Jr., Fragniere, A., Tyers, P., Jessberger, S., Saksida, L.M., Barker, R.A., Gage, F.H., and Bussey, T.J. (2009). A functional role for adult hippocampal neurogenesis in spatial pattern separation. Science *325*, 210–213.

De Vries, H. (1958). Atomic bomb effect: variation of radiocarbon in plants, shells, and snails in the past 4 years. Science *128*, 250–251.

Eisch, A.J., and Petrik, D. (2012). Depression and hippocampal neurogenesis: a road to remission? Science *338*, 72–75.

Eriksson, P.S., Perfilieva, E., Björk-Eriksson, T., Alborn, A.M., Nordborg, C., Peterson, D.A., and Gage, F.H. (1998). Neurogenesis in the adult human hippocampus. Nat. Med. *4*, 1313–1317.

Fallon, S.J., Guilderson, T.P., and Brown, T.A. (2007). CAMS/LLNL ion source efficiency revisited. Nucl Instrum Meth B *259*, 106–110.

Ge, S., Yang, C.H., Hsu, K.S., Ming, G.L., and Song, H. (2007). A critical period for enhanced synaptic plasticity in newly generated neurons of the adult brain. Neuron *54*, 559–566.

Göritz, C., and Frisén, J. (2012). Neural stem cells and neurogenesis in the adult. Cell Stem Cell *10*, 657–659.

Harkness, D.D. (1972). Further investigations of the transfer of bomb 14 C to man. Nature *240*, 302–303.

Hua, Q., Zoppi, U., Williams, A., and Smith, A. (2004). Small-mass AMS radiocarbon analysis at ANTARES. Nucl. Instrum. Methods *223-224*, 284–292.

Imayoshi, I., Sakamoto, M., Ohtsuka, T., Takao, K., Miyakawa, T., Yamaguchi, M., Mori, K., Ikeda, T., Itohara, S., and Kageyama, R. (2008). Roles of continuous neurogenesis in the structural and functional integrity of the adult forebrain. Nat. Neurosci. *11*, 1153–1161.

Jabès, A., Lavenex, P.B., Amaral, D.G., and Lavenex, P. (2010). Quantitative analysis of postnatal neurogenesis and neuron number in the macaque monkey dentate gyrus. Eur. J. Neurosci. *31*, 273–285.

Kempermann, G. (2012). New neurons for 'survival of the fittest'. Nat. Rev. Neurosci. *13*, 727–736.

Kempermann, G., Kuhn, H.G., and Gage, F.H. (1997). Genetic influence on neurogenesis in the dentate gyrus of adult mice. Proc. Natl. Acad. Sci. USA *94*, 10409–10414.

Kempermann, G., Gast, D., Kronenberg, G., Yamaguchi, M., and Gage, F.H. (2003). Early determination and long-term persistence of adult-generated new neurons in the hippocampus of mice. Development *130*, 391–399.

Kheirbek, M.A., Klemenhagen, K.C., Sahay, A., and Hen, R. (2012). Neurogenesis and generalization: a new approach to stratify and treat anxiety disorders. Nat. Neurosci. *15*, 1613–1620.

Knoth, R., Singec, I., Ditter, M., Pantazis, G., Capetian, P., Meyer, R.P., Horvat, V., Volk, B., and Kempermann, G. (2010). Murine features of neurogenesis in the human hippocampus across the lifespan from 0 to 100 years. PLoS ONE *5*, e8809.

Kohler, S.J., Williams, N.I., Stanton, G.B., Cameron, J.L., and Greenough, W.T. (2011). Maturation time of new granule cells in the dentate gyrus of adult macaque monkeys exceeds six months. Proc. Natl. Acad. Sci. USA *108*, 10326–10331.

Kornack, D.R., and Rakic, P. (1999). Continuation of neurogenesis in the hippocampus of the adult macaque monkey. Proc. Natl. Acad. Sci. USA *96*, 5768–5773.

Levin, I., and Kromer, B. (2004). The tropospheric 14CO2 level in mid latitudes of the northern hemisphere (1959-2003). Radiocarbon *46*, 1261–1272.

Levin, I., Naegler, T., Kromer, B., Diehl, M., Francey, R.J., Gomez-Pelaez, A.J., Steele, L.P., Wagenbach, D., Weller, R., and Worthy, D.E. (2010). Observations and modelling of the global distribution and long-term trend of atmospheric 14CO2. Tellus *62*, 26–46.

Libby, W.F., Berger, R., Mead, J.F., Alexander, G.V., and Ross, J.F. (1964). Replacement Rates for Human Tissue from Atmospheric Radiocarbon. Science *146*, 1170–1172.

Miller, S.A., Dykes, D.D., and Polesky, H.F. (1988). A simple salting out procedure for extracting DNA from human nucleated cells. Nucleic Acids Res. *16*, 1215.

Nakashiba, T., Cushman, J.D., Pelkey, K.A., Renaudineau, S., Buhl, D.L., McHugh, T.J., Rodriguez Barrera, V., Chittajallu, R., Iwamoto, K.S., McBain, C.J., et al. (2012). Young dentate granule cells mediate pattern separation, whereas old granule cells facilitate pattern completion. Cell *149*, 188–201.

Ninkovic, J., Mori, T., and Götz, M. (2007). Distinct modes of neuron addition in adult mouse neurogenesis. J. Neurosci. *27*, 10906–10911.

Nydal, R., and Lövseth, K. (1965). Distribution of radiocarbon from nuclear tests. Nature *206*, 1029–1031.

Rakic, P. (1985). Limits of neurogenesis in primates. Science *227*, 1054–1056.

Sahay, A., Scobie, K.N., Hill, A.S., O'Carroll, C.M., Kheirbek, M.A., Burghardt, N.S., Fenton, A.A., Dranovsky, A., and Hen, R. (2011). Increasing adult hippocampal neurogenesis is sufficient to improve pattern separation. Nature *472*, 466–470.

Salehpour, M., Hakansson, K., and Possnert, G. (2013). Accelerator mass spectrometry of ultra-small samples with applications in the biosciences. Nucl Instrum Meth B *294*, 97–103.

Sanai, N., Nguyen, T., Ihrie, R.A., Mirzadeh, Z., Tsai, H.H., Wong, M., Gupta, N., Berger, M.S., Huang, E., Garcia-Verdugo, J.M., et al. (2011). Corridors of migrating neurons in the human brain and their decline during infancy. Nature *478*, 382–386.

Santos, G.M., Southon, J.R., Griffin, S., Beaupre, S.R., and Druffel, E.R.M. (2007). Ultra small-mass AMS C-14 sample preparation and analyses at KCCAMS/UCI Facility. Nucl Instrum Meth B *259*, 293–302.

Schmidt-Hieber, C., Jonas, P., and Bischofberger, J. (2004). Enhanced synaptic plasticity in newly generated granule cells of the adult hippocampus. Nature *429*, 184–187.

Spalding, K.L., Bhardwaj, R.D., Buchholz, B.A., Druid, H., and Frisén, J. (2005a). Retrospective birth dating of cells in humans. Cell *122*, 133–143.

Spalding, K.L., Buchholz, B.A., Bergman, L.-E., Druid, H., and Frisén, J. (2005b). Forensics: age written in teeth by nuclear tests. Nature *437*, 333–334.

Spalding, K.L., Arner, E., Westermark, P.O., Bernard, S., Buchholz, B.A., Bergmann, O., Blomqvist, L., Hoffstedt, J., Näslund, E., Britton, T., et al. (2008). Dynamics of fat cell turnover in humans. Nature *453*, 783–787.

Steiner, B., Kronenberg, G., Jessberger, S., Brandt, M.D., Reuter, K., and Kempermann, G. (2004). Differential regulation of gliogenesis in the context of adult hippocampal neurogenesis in mice. Glia *46*, 41–52.

Wang, C., Liu, F., Liu, Y.-Y., Zhao, C.-H., You, Y., Wang, L., Zhang, J., Wei, B., Ma, T., Zhang, Q., et al. (2011). Identification and characterization of neuroblasts in the subventricular zone and rostral migratory stream of the adult human brain. Cell Res. *21*, 1534–1550.